EDEM Contact Model: An Improved Linear Model for Elasto-Plastic and Adhesive Contact

Wenguang Nan

Nanjing Tech University

University of Leeds

1. Introduction

For a given material, the effect of plastic deformation must be accounted if the particle size is below the critical value, in which the attractive force (such as van der Waals force) itself could induce plastic deformation as long as the particles can be brought into contact. This is known as adhesion-induced plastic deformation or jump-in induced plastic deformation. A non-dimensional number is proposed to quantify this critical particle radius, given as [1]:

$$CY = \frac{p_y{}^3 R}{E^2 \Gamma} \tag{1}$$

For a given material (i.e. p_y, E, Γ is fixed), with a decrease in particle size, CY decreases, and there is a critical particle size, below which adhesion-induced plastic deformation could. Below this critical particle size, the smaller the particle size, the more cohesive the particle behaves than the one predicted by traditional JKR theory. An example of the critical particle radius is given in Nan et al. [2]: considering the fact that the yield stress of 316L stainless steel is usually 200-300 MPa, and the ratio of the yield contact pressure to yield stress is about 1.6, as well as E=211 GPa and Γ=9 mJ/m^2 [3], the critical particle diameter would be about 24.5-7.2 μm, which is overlapped with PSD of 316L stainless steel powder used in the spreading technology in additive manufacturing. Of course, plastic deformation could also have a significant effect on bulk behaviour of cohesive powder if the characteristic velocity of the particulate system or the external load is extremely large, such as jamming-induced plastic deformation in additive manufacturing [2, 3].

Based on the work of Thornton and Ning [4] and Pasha et al. [5], an improved linear model is developed for elasto-plastic and adhesive contact in DEM simulation [1]. The proposed contact model is also well validated against the numerical simulation (FEM) and experimental work in literature. This contact model is also successfully applied to the analysis of single particle impact test, as well as the DEM simulation of bulk particle behaviour in FT4 rheometer [1] and powder spreading technology in Additive Manufacturing [2]. This model has been implemented into EDEM using CPU-based API, which could also be easily transformed to GPU-based version. The proposed contact model could be

reduced to simpler case, such as elasto-adhesive contact (by setting the yield contact pressure to a very large value), elasto-plastic contact (by setting the interfacial energy to zero). It is therefore applicable for DEM simulation of most particulate systems.

2. Framework

The total contact force, $\boldsymbol{F}$, is the sum of normal contact force $\boldsymbol{f}_n$, tangential contact force $\boldsymbol{f}_t$, and the damping force ($\boldsymbol{f}_{nd}$, $\boldsymbol{f}_{td}$):

$$\boldsymbol{F}_n = \boldsymbol{f}_n + \boldsymbol{f}_{nd} \tag{2}$$

$$\boldsymbol{F}_t = \boldsymbol{f}_t + \boldsymbol{f}_{td} \tag{3}$$

2.1 Normal contact force

The normal contact force $\boldsymbol{f}_n$ is given as:

$$\boldsymbol{f}_n = f\boldsymbol{n} \tag{4}$$

where $\boldsymbol{n}$ is the unit vector in the normal direction; f is the magnitude of normal contact force, which is linear to the normal overlap α. The general mathematical form of the normal contact force for both before and after yielding is given as:

$$f = \begin{cases} \min(f_e, f_p) & \alpha > \alpha_{cp} \\ f_c & \alpha_{fp} \le \alpha \le \alpha_{cp} \\ 0 & \alpha < \alpha_{fp} \parallel cs = 0 \end{cases} \tag{5}$$

where α_{cp} is the overlap where the maximum pull-off force f_{cp} is reached; α_{fp} is the overlap where the particles in contact are detached; cs is a parameter describing the contact state: first loading with $\alpha<0$ and reloading with $\alpha<\alpha_{c0}$; f_e, f_p and f_c are the forces, given as:

$$f_e = k_e(\alpha - \alpha_p) \tag{6}$$

$$f_p = f_y + k_p(\alpha - \alpha_y) \tag{7}$$

$$f_c = -f_{cp} + k_c(\alpha_{cp} - \alpha) \tag{8}$$

where α_p is the overlap after yielding where the normal force is zero; k_e is the elastic stiffness after yielding; f_y is the yield force; k_p is the plastic stiffness; α_y is the overlap at the yielding point; k_c is the stiffness when the overlap is less than α_{cp}.

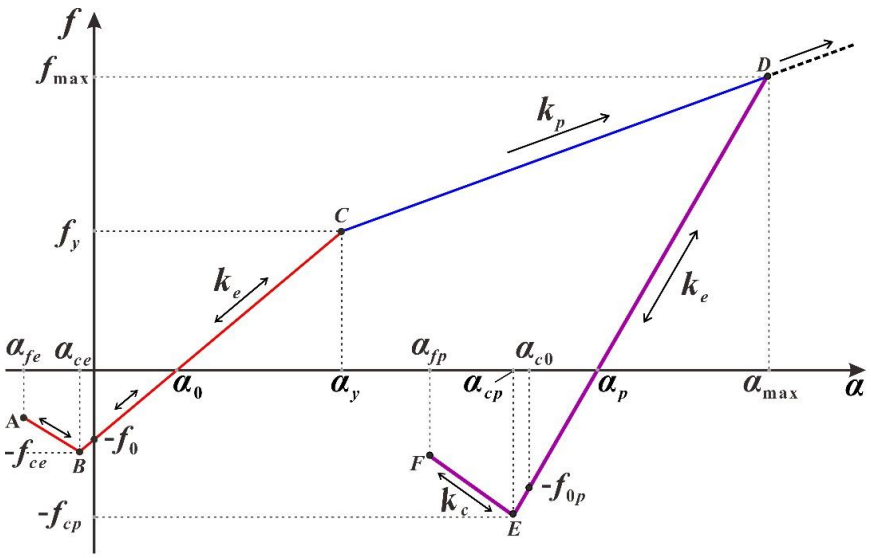

Fig. 1. Schematic diagram of the normal force *f*-overlap α relationship.

The critical normal overlaps in Fig. 1 are given as:

$$\alpha_y = \alpha_0 + \frac{f_y}{k_{el}} \tag{9}$$

$$\alpha_{\max} = \alpha_y + \frac{f_{\max} - f_y}{k_p} \quad \text{with} \quad \alpha_{\max} = \max(\alpha_{\max}, \alpha_y) \tag{10}$$

1) Before yielding:

$$\alpha_0 = \frac{f_0}{k_{el}} = \frac{8}{9}\frac{f_{ce}}{k_{el}} \tag{11}$$

$$\alpha_{ce} = \alpha_0 - \frac{f_{ce}}{k_{el}} \tag{12}$$

$$\alpha_{fe} = \alpha_0 - \frac{f_{ce}}{k_{el}} - \frac{4}{9}\frac{f_{ce}}{k_{cl}} \tag{13}$$

2) After yielding:

$$\alpha_p = (1 - \frac{k_p}{k_e})(\alpha_{\max} - \alpha_y) + (1 - \frac{k_{el}}{k_e})(\alpha_y - \alpha_0) + \alpha_0 \tag{14}$$

$$\alpha_{c0} = \alpha_p - \frac{8}{9}\frac{f_{cp}}{k_e} \tag{15}$$

$$\alpha_{cp} = \alpha_p - \frac{f_{cp}}{k_e} \tag{16}$$

$$\alpha_{fp} = \alpha_p - \frac{f_{cp}}{k_e} - \frac{4}{9}\frac{f_{cp}}{k_c} \tag{17}$$

where $\alpha_{\max}$ is the maximum overlap with force f_{max} at which the unloading commences, and it would be only immediately updated and equal to the normal overlap when the contact is yielded again, to prepare for the possible unloading process in the next time step. During the reloading stage, the contact could only be re-established at $\alpha=\alpha_{c0}$ with an initial value of $-f_{0p}$.

For the contact before yielding, $\alpha_{\max}$ in Eq. (10) is mathematically reduced to $\alpha_{\max}=\alpha_y$ while k_e is reduced to its minimum value (i.e. k_{el}), thus, Eq. (14) is reduced to $\alpha_p=\alpha_0$, and f_{cp} is reduced to $f_{cp}=f_{ce}$ (shown below), k_c is reduced to k_{cl} (shown below), resulting in $\alpha_{fp}=\alpha_{fe}$, $\alpha_{cp}=\alpha_{ce}$, and $\alpha_{c0}=0$. Therefore, Eqs. (14)-(17) could be deemed as a general mathematical form for the calculation of critical normal overlaps, which are valid for both the contacts before and after yielding.

2.2 Tangential contact force

The tangential contact force $\boldsymbol{f}_t$ is given as:

$$\boldsymbol{f}_t = k_t \boldsymbol{\delta}_t \tag{18}$$

where $\boldsymbol{\delta}_t$ is the vector of tangential displacement; k_t is tangential stiffness, which is related to k_n [6]:

$$\frac{k_t}{k_n} = 4\frac{G^*}{E^*} \tag{19}$$

where G^* and E^* are the equivalent shear modulus and Young's modulus, respectively; k_n is the normal stiffness, i.e. k_c for line AB or EF, k_e for line BC or DE, k_p for line CD, as shown in Fig. 1. For the sliding contact, i.e. $k_t|\boldsymbol{\delta}_t|>\mu f$, the energy is dissipated from the interfacial sliding without introducing the viscous damping in the tangential direction. Thus, Eq. (3) is reduced to $\boldsymbol{F}_t=\boldsymbol{f}_t$, given as:

$$\boldsymbol{F}_t = \mu f \frac{\boldsymbol{\delta}_t}{|\boldsymbol{\delta}_t|} \tag{20}$$

where μ is the sliding friction coefficient; f is normal force in Eq. (5).

2.3 Damping force

For the contact before yielding, besides the frictional dissipation through interfacial sliding and adhesive work, the energy dissipation is mainly attributed to the viscous elastic damping, especially in the normal direction. The damping force in the normal and tangential direction is given as:

$$\boldsymbol{f}_{nd} = 2\gamma\sqrt{m^* k_n}\boldsymbol{V}_n \tag{21}$$

$$\boldsymbol{f}_{td} = 2\gamma\sqrt{m^* k_t}\boldsymbol{V}_t \tag{22}$$

where γ is the damping coefficient due to viscous and viscoelastic damping effect or energy dissipation of elastic wave propagation; m^* is the equivalent mass; $\boldsymbol{V}_n$ and $\boldsymbol{V}_t$ are the relative velocity in normal and tangential direction, respectively. γ is related to elastic restitution coefficient e_0, given as:

$$\gamma = -\beta\frac{\ln e_0}{\sqrt{\pi^2 + (\ln e_0)^2}} \tag{23}$$

where β=1 is the damping factor.

For the contact after yielding, the energy dissipation of elastic wave propagation during impact is very small, compared to the ones due to plastic deformation, as reported by Ning et al. [7], indicating that viscous elastic damping could be ignored (i.e. β=0). However, in the impact test, if the viscous damping force is omitted while the particle could not rebound, the contact force oscillates indefinitely along line D-E-F (Fig. 1), and a state of equilibrium can never be achieved as no energy is dissipated. Meanwhile, the material is not perfectly plastic. Therefore, a small value of β (e.g. 0.1) is necessary, although its contribution to total energy dissipation can be ignored.

2.4 Time step

The critical time step is given as:

$$\frac{\Delta T_{crit}}{\Delta T_R} = \frac{0.1631\upsilon + 0.8766}{\sqrt{1+\upsilon}}\sqrt{\frac{4}{3\pi}}\left(\frac{\alpha_{\max}}{R}\right)^{-1/4} \tag{24}$$

$$\Delta T_R = \frac{\pi R}{0.1631\upsilon + 0.8766}\sqrt{\frac{\rho}{G}} \tag{25}$$

where ΔT_R is critical time step based on Rayleigh surface wave in traditional contact model. As the maximum normal overlap is usually less than $0.1R$ and $\Delta T_{\text{crit}}/\Delta T_R$ is inversely proportional to α_{max}/R, $\Delta T_{\text{crit}}/\Delta T_R$ could be roughly assumed to be 1 for most particulate systems. Therefore, the time step in DEM simulation for the contact model developed in this work could also be evaluated from the Rayleigh time step in Eq. (25).

It should be noted that the above analysis only provides the maximum limit of the time step, as it

does not consider the details of the contact process. Thus, the value of time step used in DEM simulation should be evaluated based on the particulate systems. For most simulation systems, Δt=(0.1~0.25)ΔT_R can be adopted for a good balance between the computational time and accuracy, which is similar to the cases using Hertz contact model [6]. For particulate systems with high collision velocity, e.g. impact of particle against a wall, to accurately detect the contact details (e.g. the line EF in Fig.1), much smaller time step is conservatively suggested, e.g. Δt=0.01~0.1ΔT_R.

3. Key parameters

The correlations to estate the key parameters, i.e. yield point (f_y, α_y), stiffness (k_e, k_c, k_p) and maximum pull-off force (f_{cp}), could be derived based on the work of deformation. The physical nature of contact is well kept during the derivation, and the correlations are validated against the data extracted from the literature. Details could be found in Nan et al. [1], and a brief summary of the correlations are shown below.

3.1 Contact force and normal overlap at yield point, f_y and α_y

The yield force and the corresponding normal overlap are given as:

$$f_y = f_{y0}\sqrt{\frac{6}{5}\frac{k_{el}}{\pi R^* p_y}} \tag{26}$$

$$\alpha_y - \alpha_0 = \frac{f_y}{k_{el}} = \alpha_{y0}\sqrt{\frac{8}{15}\frac{\pi R^* p_y}{k_{el}}} \tag{27}$$

where f_{y0} and α_{y0} are the yield force and the corresponding normal overlap predicted by Thornton and Ning [4] in their non-linear contact model:

$$f_{y0} = \frac{\pi^3 R^{*2} p_y^{\ 3}}{6E^{*2}} \tag{28}$$

$$\alpha_{y0} = \frac{\pi^2 R^* p_y^{\ 2}}{4E^{*2}} \tag{29}$$

where p_y is the limiting contact pressure of the softer particle, i.e. p_y=min(p_{y1}, p_{y2}) . p_y is related to the yield stress σ_y, i.e. p_y/σ_y=1.4~1.7 for most particulate systems.

3.2 Stiffness k_c

The ratio of k_e/k_c after yielding is assumed to follow the same law as k_{el}/k_{cl} before yielding:

$$\frac{k_{el}}{k_{cl}} = 1.13\frac{k_{el}}{k_{H-JKR,\,\alpha=0}} - 0.3 \tag{30}$$

$$k_{H-JKR,\,\alpha=0} = 1.23(\Gamma E^{*2} R^{*2})^{1/3} \tag{31}$$

where $k_{H\text{-}JKR,\,\alpha=0}$ is the normal stiffness at α=0 predicted by Hertz model with JKR theory

3.3 Stiffness k_e

1) Method A:

Based on the given unloading line after yielding, i.e. k_{e0} at $\alpha_{\max 0}$ is known, stiffness k_e is given as:

$$k_e = k_{e0}\sqrt{\frac{\alpha_{\max}}{\alpha_{\max 0}}} \tag{32}$$

For the contact before yielding, i.e. $\alpha<\alpha_y$ for line BC, k_{el} is the lower limit of k_e, and it is calculated by substituting $\alpha_{\max}= \alpha_y$ into Eq. (32), given as:

$$k_{el} = k_e(\alpha_{\max} = \alpha_y) = k_{e0}\sqrt{\frac{\alpha_y}{\alpha_{\max 0}}} \tag{33}$$

As α_y is a function of k_{el}, Eq. (33) should be solved together with Eq. (27) in an iterative fashion by initially assuming $\alpha_y=\alpha_{y0}$.

2) Method B:

The elastic stiffness k_e can also be evaluated through the stiffness of the contact before yielding, i.e. k_{el} for line BC in Fig. 1 is known. In this case, α_y can be directly calculated from Eq. (27). Similar to Eq. (32), the elastic stiffness k_e for line DE in Fig. 1 is given as:

$$k_e = k_{el}\sqrt{\frac{\alpha_{\max}}{\alpha_y}} \tag{34}$$

3) Method C:

If there are no experimental data available for the input parameters, i.e. k_p, and k_{el} (or $\alpha_{\max 0}$ and k_{e0}), the following value is recommended for k_{el}, and k_p could be assumed to be the same as k_{el}.

$$k_{el} = 2E^*\sqrt{R^*\alpha_{y0}} = \pi R^* p_y \tag{35}$$

3.4 Maximum pull-off force f_{cp}

The maximum pull-off force f_{cp} is given as:

$$\frac{f_{cp}}{f_{ce}} = \frac{-A + \sqrt{A^2 + 4\frac{k_e}{k_{el}}\left(\frac{\alpha_p}{\alpha_0}A + 1\right)}}{2} \tag{36}$$

where A is constant for each contact pair and could be given as:

$$A = \frac{\frac{16}{27}}{\frac{56}{162}\frac{k_e}{k_c} + \frac{17}{162}} \tag{37}$$

4. Input parameters

In the contact model developed in this work, several parameters are involved, but most of them can be calculated based on the contact properties of single particle. For example, f_y from Eq. (26), α_y from Eq. (27), k_c from Eq. (30) for the contact after yielding, f_{cp} from Eq. (36). Thus, apart from the particle properties and interaction parameters in conventional contact models (i.e. Hertz-Mindlin model), such as Young's modulus, friction coefficient, etc., there are only four additional input parameters:

Surface Energy, Γ (J/m^2): It can be experimentally measured from the drop test [8]. However, for particle with large surface energy and small yield contact pressure, the experiment test could lead to large error (i.e. the contact is already yield during the test). In this case, surface energy Γ can be roughly estimated from Hamaker constant of material and then further calibrated by DEM simulation of bulk particle flow.

Yield Pressure, p_y (Pa): It could be preferentially calculated from the yield stress σ_y of materials. The yield stress here is referred to the compressing yield stress instead of the pulling yield stress. Usually, σ_y/E is 0.001~0.1 for most materials. As the state of the contact (yield or not) is strongly determined by the yield contact pressure, σ_y should be carefully examined or calibrated.

Stiffness k_{el} and k_p: plastic stiffness k_p is calculated directly from the loading curve in the experiment, while lower limit of elastic stiffness k_{el} could be calculated by Eq. (33) with k_{e0} and $\alpha_{\max 0}$

extracted from unloading curve, where large loading force is needed to yield the contact in the indentation test. If no experimental data of the loading/unloading curves is available, k_{el} can be estimated from yield contact pressure p_y using Eq. (35), and k_p can be assumed to be the same as k_{el}. By default, the lower limit of elastic stiffness $k_{el} = \pi R^* p_y$.

5. Advantages

Compared to the non-linear model of Thornton and Ning [4], the linear models of Pasha et al. [5] and Luding [9], the newly developed model shows several improvements in terms of physical nature and computational time, which are described in detail below and summarised in Table 1.

The proposed model in this work is a linear version of the non-linear model of Thornton and Ning [4], but its physical nature is well kept. For example, both the adhesive sticking velocity predicted by JKR theory and plastic work predicted by plasticity theory are guaranteed in the proposed contact model. The governing equations of the non-linear model of Thornton and Ning [4] are in a very complex form. Compared to Thornton and Ning's model, the proposed contact model has a significant advantage in terms of much less computational time and easily implementation into DEM software package. For example, for the particulate system in FT4 rheometer shown in Nan et al. [1], the total computational time using the newly developed model (512 minutes) is on par with EDEM Built-in JKRV2 model (514 minutes), where 73, 577 particle and 10 CPU cores on DELL PowerEdge T640 workstation are involved.

The proposed contact model has several additional advantages: 1) Compared to Pasha et al. [5], thorough unified mathematical equations are formally presented here, making it easy for implementation in DEM software packages with low computational time, while no similar mathematical framework could be accessed in Pasha et al. [5]. 2) Compared to Luding [9] where plastic deformation is assumed to be present from the beginning, both the initial elastic and plastic deformation could be considered here, making it more realistic, i.e. in dynamic particulate systems, the external load applied on the particles at some regions is not large enough to cause yielding, and

hence the contact is still elastic. 3) The number of parameters required for experimental characterisation in the proposed contact model is minimised. For example, compared to Hertz model with JKR theory, only the yield stress is additionally required in some cases, which could be easily found in the handbook of materials. On the contrast, the models Pasha et al. [5] and Luding [9] involves a number of key parameters which is not accessible from single particle characterisation.

Table 1. Comparisons of the contact model for the elasto-plastic and adhesive contact.

Contact model	Thornton & Ning [4]	Pasha et al. [5]*	Luding [9]	This work
Computational time and complexity	High	Low	Low	Low
Unified mathematical equations	Provided	/	Provided	Provided
Ability to consider both elastic and plastic deformation in dynamic particulate system	Yes	Yes	/	Yes
Rigorous equations to calculate the key parameters	Provided	/	/	Provided
Method to calculate critical sticking velocity considering both elastic and plastic deformation	Part-provided**	/	/	Provided

* It is referred to the full model instead of the simplified version in Pasha et al. [5].

** Effect of elastic and plastic deformation on critical sticking velocity is discussed separately in Thornton & Ning [4].

References

[1] W. Nan, W.P. Goh, M.T. Rahman, Elasto-plastic and adhesive contact: An improved linear model and its application, Powder Technology, 407 (2022).

[2] W. Nan, M.A. Rahman, L. Ge, Z. Sun, Effect of plastic deformation on the spreadability of cohesive powder in the spreading process, Powder Technology, 425 (2023).

[3] W. Nan, M. Pasha, T. Bonakdar, A. Lopez, U. Zafar, S. Nadimi, M. Ghadiri, Jamming during particle spreading in additive manufacturing, Powder Technology, 338 (2018) 253-262.

[4] C. Thornton, Z. Ning, A theoretical model for the stick/bounce behaviour of adhesive, elastic-plastic spheres, Powder Technology, 99 (1998) 154-162.

[5] M. Pasha, S. Dogbe, C. Hare, A. Hassanpour, M. Ghadiri, A linear model of elasto-plastic and adhesive contact deformation, Granular Matter, 16 (2014) 151-162.

[6] C. Thornton, Granular Dynamics, Contact Mechanics and Particle System Simulations, Springer, New York, 2015.

[7] Z. Ning, Elasto-Plastic Impact of Fine Particles and Fragmentation of Small Agglomerates, Aston University, 1995.

[8] U. Zafar, C. Hare, A. Hassanpour, M. Ghadiri, Drop test: A new method to measure the particle adhesion force, Powder Technology, 264 (2014) 236-241.

[9] S. Luding, Cohesive, frictional powders: contact models for tension, Granular Matter, 10 (2008) 235-246.